



PARAMETRIC STUDY FOR OPTIMIZATION OF THE ICE TUBE GENERATOR OF LABORATORY

ESTUDIO PARAMÉTRICO PARA OPTIMIZACIÓN DE UN GENERADOR DE HIELO TUBULAR DE LABORATORIO

Rocío Guapulema-Maygualema^{1,*}, Víctor Hidalgo-Díaz^{2,3}

Abstract

In Ecuador, there is a large energy consumption by air conditioning and refrigeration in the industrial, commercial and residential sectors. A maximum electricity demand reduction method is to incorporate an optimal cooling thermal energy storage system. The main objective of this work was to develop a parametric study of laboratory ice tube generator for an after optimization. For that, the main parameters were studied, which are: water storage temperature, refrigerant temperature in the evaporator and condenser, ice subcooling temperature and ice formation speed. Two outstanding parameters that intervened in the ice formation process were the place environmental conditions and the water temperature used, when the environmental temperature decreased, thermal load also decreased and condenser efficiency improved, which directly influenced the efficiency of the equipment. The instability observed in the first hour of test intervened in the final water temperature, final temperature ranged from 1.1 °C to -0.4 °C in three hours.

Keywords: Energy efficiency, ice, bank, optimization, refrigeration, storage.

Resumen

En Ecuador existe un gran consumo energético por climatización y refrigeración en los sectores industrial, comercial y residencial. Un método para reducir la demanda eléctrica máxima es incorporar un sistema óptimo de almacenamiento de energía térmica de refrigeración. Este trabajo tiene por objetivo realizar el estudio paramétrico de un generador de hielo tubular de laboratorio para su posterior optimización. Se estudiaron los principales parámetros que intervienen en la formación de hielo como temperatura del agua en el reservorio, temperaturas del refrigerante en el evaporador y condensador, temperatura de subenfriamiento del hielo y velocidad de formación de hielo. Los parámetros destacados que intervinieron en el proceso fueron las condiciones ambientales del lugar y la temperatura del agua utilizada. Al disminuir la temperatura ambiental, disminuye la carga térmica y mejora la eficiencia del condensador, el cual influye directamente sobre la eficiencia del equipo. La inestabilidad observada en la primera hora de prueba intervino en la temperatura final del agua, la misma que varió en el rango de 1,1 °C a -0,4 °C en 3 horas.

Palabras clave: eficiencia energética, generador, hielo, optimización, refrigeración, almacenamiento.

^{1,*}Faculty of Land Sciences and Water, Universidad Regional Amazónica Ikiam, Tena 150150, Ecuador. Corresponding author ✉: rocio.guapulema@ikiam.edu.ec, r.guapulema@hotmail.com

<http://orcid.org/0000-0002-2768-9018>

²Department of Mechanical Engineering, Escuela Politécnica Nacional, Quito 170525, Ecuador.

<http://orcid.org/0000-0003-4732-2421>

³Laboratory of Informatics-Mechanics, Escuela Politécnica Nacional, Quito 170525, Ecuador.

Received: 24-10-2019, accepted after review: 09-12-2019

Suggested citation: Guapulema-Maygualema, R. and Hidalgo-Díaz, V. (2020). «Parametric Study for Optimization of the Ice Tube Generator of Laboratory». INGENIUS. N.º 23, (january-june). pp. 86-96. DOI: <https://doi.org/10.17163/ings.n23.2020.08>.

1. Introduction

Nowadays, saving energy and protecting the environment are important issues worldwide [1]. On the other hand, the storage of thermal energy is considered one of the most important energy technologies [2] for reducing electrical consumption. Studies on ice generators have been carried out with the purpose of evaluating and improving its operation for reducing electrical consumption; parameters evaluated such as thermal conductivity of the material of the condenser, tank capacity, longitudinal and cross pitches of the condenser tube and coolant temperatures [3], directly affect the design of the equipment, space requirement and efficiency of the system. Similarly, energy losses due to ice storage, cost structure and electricity tariffs, periods of tariffs, storage capacity of ice generators and impact of load prevision, have been also evaluated [4].

A model for the optimization of air conditioning systems with thermal accumulation and system simulation results are presented in [5]. Considering that the growing demand of air conditioning systems has led to a greater energy consumption during peak hours [6], thermal energy storage systems are becoming increasingly popular [7], enabling to conduct studies about physical, technical, economic, environmental [8,9] and raw material consumption [10] aspects of thermal energy storage refrigeration systems and their applications [2], with the purpose of finding a method to improve their efficiency [11].

In Ecuador, the residential, industrial and commercial sectors represent the 31 %, 25.9 % and 15.9 %, respectively, of the energy demand [12]; approximately 50 % of the energy consumption in the residential and commercial sectors of the Costa and Sierra regions is due to cooling and conditioning [13]. The National Balance of Electric Energy presented in June 2019 by the Agency for Electricity Regulation and Control (in Spanish ARCONEL, Agencia de Regulación y Control de Electricidad), indicates that the electricity consumption by these sectors was 17736.87 GWh [12]. A method for reducing the maximum demand of electricity is incorporating storage of thermal energy for refrigeration [14], in order to transfer the energy consumption at peak hours to the hours of low consumption [7, 10, 15]. The thermal energy may be stored using sensible or latent heat [16, 17], namely, cold water or ice, the latter being advantageous since it requires smaller storage volumes [18, 19].

With the purpose of saving energy and optimizing processes which use storage of refrigeration energy, namely conditioning, dairy processing, breweries, plastics manufacturing and chemical processes, among others, it is important to simulate the efficiency that an equipment for generating and storing ice would have. A parametric study was carried out for the optimization of the tubular ice generator constructed in the

project entitled Design and construction of a laboratory tubular ice generator [20]. This generator, which corresponds to a system of ice on evaporator, consists of an arrangement of tubes submerged in a tank and through which cold coolant is pumped to freeze the water around them [21]. The parameters that intervene in the process of ice formation and storage of thermal energy for cooling, were studied by means of the mathematical modeling of the thermal and heat transfer cycle. A program was created in the Guide environment of Matlab for numerically simulating the operation of the equipment in different conditions, while an experimental study was conducted to assess the numerical simulation. The most important parameters that modify the operation and efficiency of the generator were defined through this study.

The parameters under consideration for the study include the water storage temperatures in the generator, temperatures of the coolant in the evaporator and condenser, ice subcooling temperature, ice thickness and speed of releasing and extracting the heat in a natural manner. It was important to study the generation of ice, taking into account that as the thickness increases, the resistance of heat transfer also increases [22, 23].

2. Materials and methods

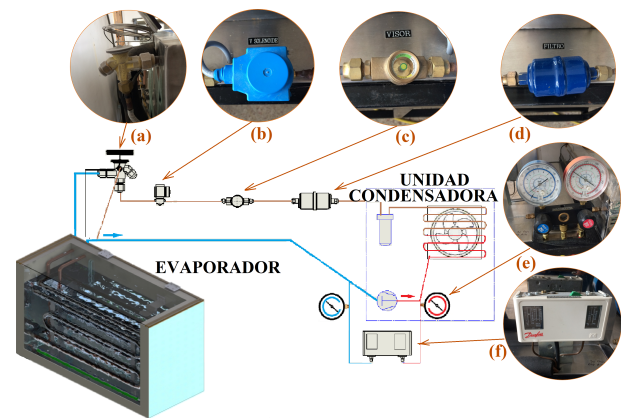


Figure 1. Laboratory tubular ice generator and its constituting elements: a) expansion valve, b) solenoid valve, c) liquid viewer, d) drying filter, e) pressures gauges, f) pressure switch

The equipment used for the parametric study is constituted by a condensing unit L'UNIQUE HERMETIQUE CAJ2428ZBR of capacity 1/2 HP, which uses R404a as coolant, a TES 2-0.45 expansion valve, a A-TD -132 SAE filter, a SGI-10 liquid viewer, a TR ¼ 032F8107 solenoid valve, pressure switch, pressure gauges, control board, tank-reservoir set, air system for water agitation and an evaporator housed in the tank (Figure 1), which is constituted by two type L copper coils with a diameter of 15.88 mm (1/2 in.),

and each with a length of 3 m. The spacing between the coils is 120 mm.

In addition, the elements in the data acquisition system include the control interface, LM 35 sensors, Arduino UNO boards, computer and software for data acquisition.

2.1. Mathematical modeling of the ice generation

2.1.1. analysis of the thermal cycle

The process for the study and evaluation of the cooling cycle and its efficiency is indicated in [24]. This information was considered as the base for the mathematical modeling of the cooling cycle.

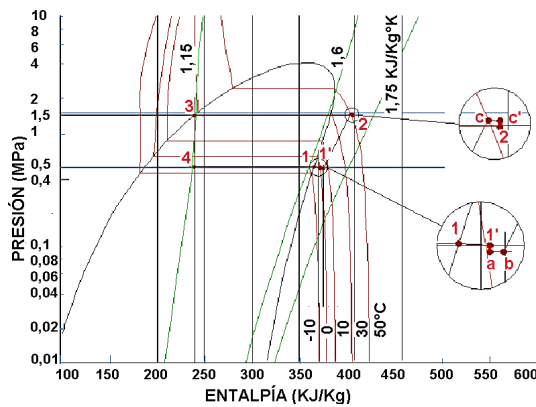


Figure 2. Pressure-Enthalpy Diagram of the tubular ice generator.

Four processes can be observed in the Pressure-Enthalpy diagram (Figure 2). The coolant that ideally can be found as saturated steam at a temperature $T_1 = -0.5^\circ\text{C}$, is compressed and reheated until it reaches condensation conditions at a pressure $P \approx 1,416 \text{ MPa}$ and at a temperature $T \approx 28,9^\circ\text{C}$, and subsequently condensed without temperature variation. Afterwards it passes through an expansion valve, where the pressure and temperature decrease and the enthalpy is maintained, later absorbing heat in the reservoir and changing its state from liquid to gas.

The real enthalpy h'_1 is calculated using the equation of the change of enthalpy at constant pressure shown in Equation 1.

$$h'_1 = h(T'_1, P_1) = h(T_1, P_1) = h(T_1, P_1) + \int_{T_1}^{T'_1} C_{p_{ref}} dT \quad (1)$$

where T'_1 and P_1 represent the real temperature and the pressure at point 1, respectively, and $C_{p_{ref}}$ is the specific heat of the coolant.

The pressure drop in the suction valve towards the compressor is evaluated at point a, and the enthalpy is calculated by means of the equation of change

of enthalpy at constant temperature, as indicated in Equation 2.

$$h_a = h(T'_1, P'_1) + \int_{P'_1}^{P_a} \left[v_a - T_a \frac{R_{ref}}{P'_1} \right] dT \quad (2)$$

where R_{ref} is the constant of the coolant, P'_1 is the real pressure at point 1, and v_a and T_a are the specific volume of the coolant and the temperature at point a, respectively.

It is considered a pressure drop at the outlet of the condenser, due to the effect of the friction of the coolant as it passes through this component. Equation 3 is used for calculating the enthalpy of the coolant on the line of constant entropy, considering an isentropic compression process.

$$h_c = c_1 + c_2(T_c - T_b) + c_3(T_c - T_b)^2 + c_4(T_c - T_b)^3 + h_b \quad (3)$$

where, c_1, c_2, c_3, c_4 are coefficients calculated according to the ASHRAE tables of the R404a coolant [25], T_b and T_c are saturation temperatures of the coolant as vapor at pressures and , and is the enthalpy evaluated through the contact of the coolant with the internal surface of the compressor. For points 1, b, c', 2, 3 and 4 in Figure 2, the calculation of the enthalpies is carried out according to the table of properties of the coolant.

The refrigeration efficiency of the system, the performance coefficient as a function of the useful cooling effect and the net energy supplied by the compressor are evaluated, while the amount of coolant supplied in the equipment is calculated as a function of the capacity \dot{Q} of the condensing unit, as observed in Equation 4.

$$\dot{m}_{refrigerante} = \frac{\dot{Q}}{h_b - h_4} \quad (4)$$

2.1.2. Analysis of heat transfer

Three basic situations were considered for the model:

- 1) Flow of environmental heat into the tank: The heat flows from a hot source to a cold source [26, 27], in other words, if the tank contains water at low temperature and ice on the evaporator, the heat will be transferred by free convection of the air towards the external walls of the tank, this being the first stage of the phenomenon. In the second stage, heat is transferred by conduction from the external walls of the tank to the isolation layer, and subsequently to the internal walls until reaching the water; here the transfer is studied as free convection.

- 2) Cooling of the water without formation of ice: Heat is transferred from the water to the coolant in two stages: transfer of free heat between the water and the outer surface of the evaporator, and heat transfer from the outer surface to the coolant.
- 3) Formation of ice on the evaporator: Two stages are supposed in the freezing phase; the first describes the heat transfer from the water to the ice layer, while the second stage considers the transfer of heat from the superficial layer of ice to the coolant fluid.

The data necessary for evaluating the heat transfer are taken based on the filmic temperature calculated as a function of the surface temperature T_s , and the temperature of the fluid T_∞ .

The increase of heat due to the environment is deduced as a function of the global coefficient of heat transfer, the area A of heat transfer and the temperature variations between the outside air and the water, $T_{\infty outside_air}$ and T_{mW} , respectively.

$$\dot{Q}_{pared} = \frac{T_{\infty outside_air} - T_{mW}}{\frac{1}{h_{\infty a}} + \frac{2e_{ac}}{k_{ac}A} + \frac{e_p}{k_p A} + \frac{1}{h_{\infty W}A}} \quad (5)$$

The flow of heat that goes through the wall of the tank is defined by Equation 5, where e_{ac} is the thickness of the 304 stainless steel sheet, e_p is the thickness of the polyurethane, k_{ac} is the conductivity coefficient of the 304 stainless steel, k_p represents the conductivity coefficient of the polyurethane, and $h_{\infty a}$ and $h_{\infty w}$ are the convective coefficients of the outside air and the water, respectively.

For studying the cooling of water without formation of ice, it was evaluated the coefficient $h_{\infty ref}$ of boiling forced convection, which is equal to the maximum value between the boiling coefficient h_{NBD} of the regions of dominant nucleate boiling, and the boiling coefficient of the regions of dominant convective boiling, calculated through Equations 6 and 7.

$$h_{NBD} = [0,6683Co^{-0,2}f_2(Fr_{lo}) + 1058Bo^{0,7}F_{fl}] \cdot (1-x)^{0,8}h_{lo} \quad (6)$$

$$h_{CBD} = [1,136Co^{-0,9}f_2(Fr_{lo}) + 667,2Bo^{0,7}F_{fl}] \cdot (1-x)^{0,8}h_{lo} \quad (7)$$

It was taken into account the convection number Co , the coolant friction factor f_2 , the Froude number Fr_{lo} , the boiling point Bo , the surface-fluid association parameter F_{fl} , the quality x of the coolant fluid,

the heat transfer coefficient h_{lo} ; the way to calculate these coefficients is presented in [28].

Two thermal loads were determined, \dot{Q}_{S1} that takes into account only the thermal resistance of the water, and \dot{Q}_{S2} which considers the thermal resistances of the evaporator walls and of the coolant. The two thermal loads are defined by Equations 8 and 9.

$$\dot{Q}_{s1} = 2\pi r_e L h_{\infty w} (T_{mw} - T_{s1}) \quad (8)$$

$$\dot{Q}_{s2} = \frac{T_{s1} - T_1}{\frac{\ln\left(\frac{r_e}{r_i}\right)}{2\pi k_c L} + \frac{1}{2\pi r_i L h_{\infty ref}}} \quad (9)$$

where L represents the length of the evaporator tube, r_i and r_e are the internal and external radii of the evaporator, k_c is the thermal conductivity coefficient of the copper and T_{s1} is the temperature of the water-evaporator surface layer.

The thermal load \dot{Q}_{s3} due to the heat transfer from the water to the ice surface layer (Equation 10), and the thermal load \dot{Q}_{s4} due to the heat transfer from the ice surface to the coolant (Equation 11), are calculated in the phase of formation of ice on the evaporator.

$$\dot{Q}_{s3} = 2\pi(r_e + 2e)Lh_{\infty w2}(T_{mw} - T_o) \quad (10)$$

$$\dot{Q}_{s4} = \frac{T_0 - T_1}{\frac{\ln\left(\frac{r_e+e}{r_e}\right)}{2\pi k_h L} + \frac{\ln\left(\frac{r_e}{r_i}\right)}{2\pi k_c L} + \frac{1}{2\pi r_i L h_{\infty ref}}} \quad (11)$$

where e represents the thickness of the ice formed in a time t , $h_{\infty w2}$ is the convective coefficient of the water used in the heat transfer water-evaporator, T_{mw} is the arithmetic mean of the temperatures as a function of the initial and final temperatures of the water, T_{0_water} and T_{f_agua} , respectively, and k_h is the conductivity coefficient of the ice.

The time necessary to cool the water of the reservoir from an ambient temperature to a required temperature, varies directly with respect to \dot{Q}_{s1} . Equation 12 enables the calculation of the cooling time of the water in hours, considering the mass m_{water} of the water in the tank in kg, and the specific heat of the water Cp_{agua} in $kJ/kg \text{ } ^\circ C$. The net load \dot{Q}_{neto} that the system has for water cooling and ice generation, is equal to the difference between the capacity of the condensing unit and the total load lost.

$$t_{cool_water} = \frac{1000m_{water}Cp_{water}(T_{0_water} - T_{f_water})}{3600(\dot{Q}_{net} - \dot{Q}_{s1})} \quad (12)$$

The total thickness of the ice generated in a time t (Equation 13) is determined as a function of the flow Q_{lat} of latent heat. This value results from the difference between the thermal load due to the heat transfer from the water to the surface layer of ice, and the thermal load from the ice surface to the coolant.

$$e = \frac{\sqrt{\frac{4t(Q_{lat})}{1000\pi\rho_h L h_{sf}} + D_e^2} - D_e}{2} \quad (13)$$

where D_e is the external diameter of the evaporator in meters, ρ_h is the ice density in kg/m^3 , h_{sf} is the latent heat of water fusion in kJ/kg . Meanwhile the mass m_h of ice generated is determined through Equation 14.

$$m_h = \frac{\pi}{4} ((D_e + 2e)^2 - D_e^2) L \rho_h \quad (14)$$

At an initial time the water in the tank is at ambient temperature, and with the operation of the equipment the temperature decreases until reaching a value equal or close to $0^\circ C$. The final temperature that the water will reach in a particular time, is calculated as a function of the difference between the net load and the load estimated by the thermal resistance \dot{Q}_{s1} of the water only (Equation 15).

$$T_{f_water} = T_{0_water} - \frac{t(\dot{Q}_{net} - \dot{Q}_{s1})}{m_{water} C_{p_water}} \quad (15)$$

$$T_{f2_water} = T_{0_water} - \frac{t(\dot{Q}_{net} - \dot{Q}_{s3})}{m_{water} C_{p_water}} \quad (16)$$

On the other hand, Equation 16 is used for evaluating the water temperature considering the existence of ice on the evaporator, for which it is utilized the load \dot{Q}_{s3} calculated due to the thermal resistance of the water in the freezing process.

2.2. Numerical simulation of the tubular ice generation

The program created in the Guide environment of Matlab enables the continuous modification of the data of ambient temperature and pressure, and water and coolant necessary for the thermodynamic and heat transfer analysis. Guide enabled the graphical design of the interface of the design editor, while the Matlab program to build it was automatically generated. When the changes carried out on the interface are saved, two files are created, one .fig and the other .m; the lines of code contained in the second file are the ones that create the interface in the .fig file. The program to be executed was inserted in the command zone of the push button «Calculate».

The programming sequence involves the input of type text data, which then will be converted to type double to use them in the solution of equations present in the programming, the calculation of parameters to be evaluated and the visualization of results in tables and in a graph showing the Pressure-Enthalpy diagram defined in the thermodynamic cycle. The equations

evaluated to simulate the operation of the ice generator were defined in the mathematical modeling. The interface created for the process comprises iterative cycles, for approximation of results and evaluation of the phenomenon at different values of fluid quality and of thickness of the generated ice.

Three operating scenarios were posed for the simulation, based on the morning, afternoon and night hours. This information enabled the creation of thickness variation curves, velocity of ice formation, temperature of the water in the tank and temperature of the surface layer in the evaporator.

2.3. Experimental analysis

The procedure utilized for starting-up the equipment and the data acquisition are detailed in Figure 3. The initial operating conditions of the equipment were posed when the working pressure was stabilized.

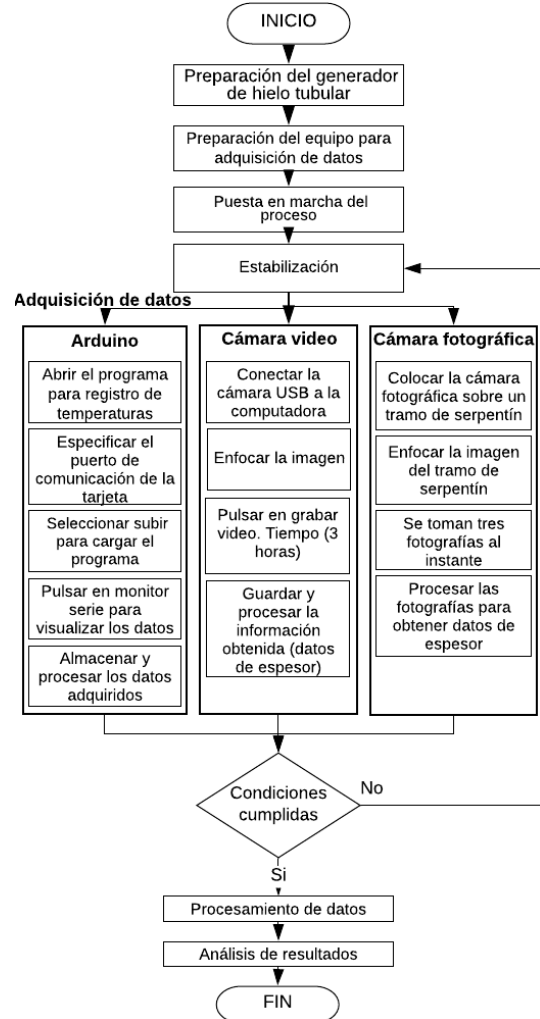


Figure 3. Process diagram of the experimental analysis.

The values of temperature at the inlet and outlet of the evaporator, at the outlet of the condenser, at the center of the reservoir and at distances of 3, 12

and 25 mm of the water-evaporator surface layer were registered. The growth of the thickness of ice was also registered using a photographic camera.

3. Results and discussion

Technical data of manufacturers and registered operating values were necessary for calculation and discussion of results. The low and high operating pressures of the system were 0.5 and 1.4 MPa (75 and 203 psig), respectively. It was determined that the coolant reaches the evaporator as a mixture of liquid and saturated steam, with a quality of 29 %. The working temperatures were $-5\text{ }^{\circ}\text{C}$ in the evaporator and $28.9\text{ }^{\circ}\text{C}$ in the condenser.

Through simulation the operating parameters were evaluated, indicating the following:

- The generation of ice in a particular time for the different experiences, started when the layer of fluid closest to the evaporator cooled until reaching the temperature of phase change, which was observed as a displacement greater than 0.2 h at the origin of each curve.
- The accelerated increase in the velocity of formation of ice and its further stabilization, represents the fast cooling that occurs in the water layers closest to the evaporator tube and its resulting freezing; lower velocities were registered as the thickness of ice was increased, with this velocity being greater in the first 1.5 h.

- The temperature of the water decreased at a rate of $7\text{ }^{\circ}\text{C}/\text{h}$ during the first two hours; beyond that time, this value decreased considerably until reaching $0.5\text{ }^{\circ}\text{C}/\text{h}$ after three hours of operation. With low ambient temperatures, the time of ice generation was smaller.
- The change in the temperature of the surface layer in the evaporator showed two variations, the first corresponding to the rate of change of the sensible heat, until reaching a temperature of $0\text{ }^{\circ}\text{C}$. Afterwards, the variation tends to stop for a range of 0.25 h; this phenomenon is due to a change of phase of the water in the zones closer to the wall of the tube. The subcooling of ice starts past the time of change of phase, until finally stabilizing at $-7\text{ }^{\circ}\text{C}$.
- An average cooling efficiency of 70 % and an average Coefficient of Performance (COP) of 5.5 were registered through numerical simulation.

Values of temperatures and thickness of ice along time were collected experimentally. Main data of the representative experiences considered for the study are detailed in Table 1.

Practices 1, 2, 3 and 4 were carried out considering natural convection of the water. On the other hand, practice 5 was carried out considering forced convection. Figure 4 shows the process of formation of ice observed in practice 2. The experimental results obtained are summarized in the following.

Table 1. Main data of the experiences under study

N.º Practice	Environment temperature $^{\circ}\text{C}$	Initial temperature of water $^{\circ}\text{C}$	Variation of temperature of condenser		Variation of pressure of condenser	
			$^{\circ}\text{C}$	$^{\circ}\text{F}$	MPa	psi
1	20,5	16	11,3	20,34	0,028	4
2	22,5	21,5	11	19,8	0,034	5
3	20	18	8,6	15,48	0,028	4
4	21,5	19,4	8,8	15,84	0,034	5
5	20	17	10,3	18,54	0,034	5

- No ice was formed in the time interval between 0 and 8 minutes. During this period, the layer of fluid closest to the evaporator cooled and then changed phase.
- The low temperature conditions resulted in a larger velocity of formation of ice, obtaining thicknesses of ice between 22 and 25 mm in 3 hours of operation.
- In an operation time greater than 3 hours, the generation of ice decreased considerably; after 5 hours of operation, the thickness of ice was approximately 35 mm, as observed in Figure5.
- The operation of the equipment in forced convection showed a faster water cooling and smaller growth of ice, compared with the results in practices in free convection.
- In a period of 5 to 10 minutes after the practice started, with a temperature $2\text{ }^{\circ}\text{C}$ smaller than the initial temperature, begins the change of phase of the fluid film closest to the evaporator. The

velocity of ice generation varied between 3 and 9 mm/h.

- The temperature of the coolant in the evaporator descends from $-3\text{ }^{\circ}\text{C}$ to $-5\text{ }^{\circ}\text{C}$, indicating the variation of the refrigeration capacity of the equipment according to the demand at that instant.

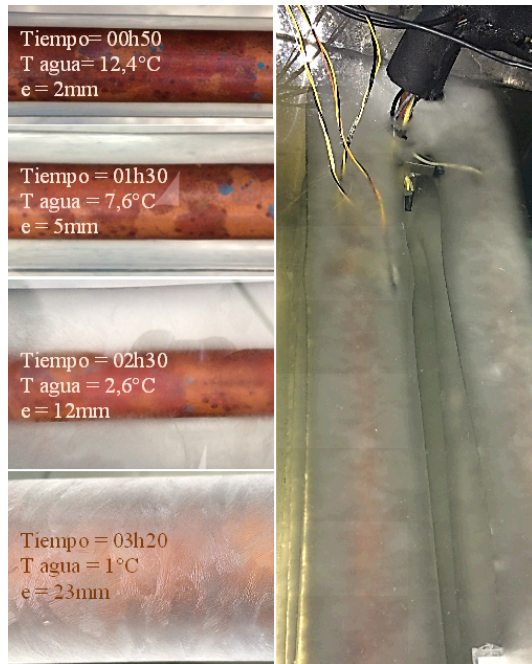


Figure 4. Thickness of ice at different time intervals. Practice 2.

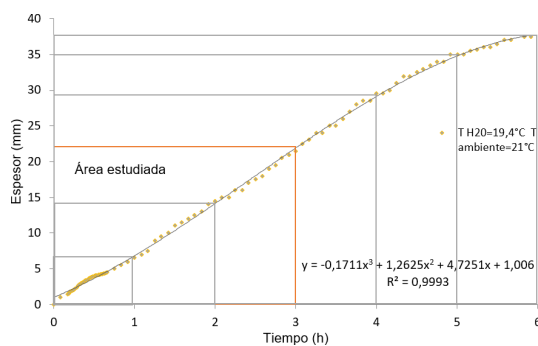


Figure 5. Thickness of ice vs. Time $T_{H20}=19.4\text{ }^{\circ}\text{C}$.

- The temperature of the coolant at the outlet of the condenser stabilizes after 15 minutes of turning on the equipment, in a range from $28\text{ }^{\circ}\text{C}$ to $34\text{ }^{\circ}\text{C}$. This value is a function mainly of the ambient temperature, temperature of the water and high pressure of the system considering the existing losses.

- The value of the total thermal load was obtained as the sum of the sensible heat and the latent heat for a particular time instant, considering the data of temperature of the water in the tank, the mass of ice and the mass of water; this value reaches an equilibrium point when the slopes of the curves of flow of sensible and latent heat have approximate values, namely, when the thermal load necessary to cool the water decreases in the same proportion in which the thermal load increases for ice generation and subcooling. It was not observed a significant variation of the thermal load past 1.5 h of operation. After 3 hours, the total thermal load varies in the range from 858 W to 892 W. In Figure 6 a), the two highest peaks (greatest thermal loads) are the result of experiences carried out in the afternoon, while the two following peaks are the result of experiences carried out at night, indicating a direct relationship with the ambient temperature and the temperature of the water.

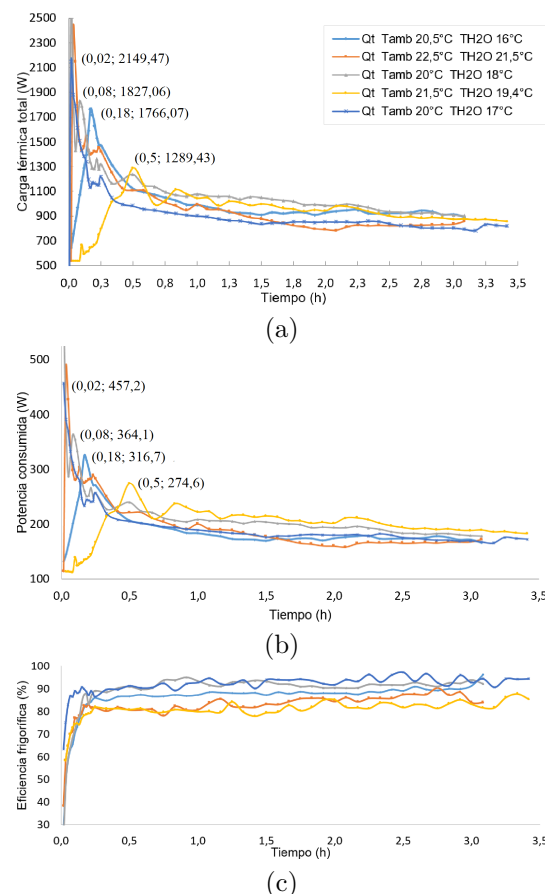


Figure 6. Experimental results. a) Total thermal load vs. time. b) Power consumed by the compressor vs. time. c) Refrigeration efficiency vs. time.

- The values of thermal load obtained between 0 and 0.5 hours are greater than the obtained 3

hours later. The peaks observed in the curves are due to the requirement of more refrigeration capacity for cooling water. At 10 minutes of operation of the equipment, 90 % of the total required refrigeration capacity corresponds to the heat necessary for water cooling, but at 3 hours of equipment operation, 40 % of the required refrigeration capacity is used for water cooling.

- The consumption of the compressor in 3 hours of operation varied in the range from 165 W to 173 W, to remove a thermal load between 859 W and 892 W. The curves shown in Figure 6 b) indicate the variation of the power consumed by the compressor according to the required refrigeration capacity.
- For each watt consumed by the compressor, approximately 5 W of thermal energy were removed from the water in the reservoir tank.
- The COP observed for different ambient temperatures and temperatures of the water varies in the range from 5.8 to 6.1, while the refrigeration efficiency fluctuates between 78 % and 95 %.
- The smallest thermal load removed was 794.11 W, obtained for the experiment carried out at an initial temperature of the water of 17 °C and ambient temperature of 20 °C in forced convection; for this experiment, the final temperature of the water was 0 °C, the COP obtained was 5.92 and the refrigeration efficiency was 90.7 % (Figure 6c). If these values are compared with the results obtained in the experiment carried out with the lowest initial temperature of the water (natural convection), the power absorbed, COP and refrigeration efficiency are very similar, whilst, when setting equal the values of final temperature of water and thickness of ice, there are important differences of -0,4 °C and 5 mm, respectively. As a consequence, using forced convection in the water improved the refrigeration efficiency of the equipment, as indicated in [11], but operating the equipment in conditions such as the observed in the practice carried out at an initial temperature of water of 16 °C resulted the best option.

A validation of the experimental results was carried out with the purpose of observing the percentage of error of the data generated with the model developed. Data from practice 1 were considered.

Figure 7a presents the variation of the water temperature water obtained by simulation and experimentally. The curve obtained by simulation is very similar to the temperature data obtained in the experiment. A water temperature of 12.8 °C was obtained 10 minutes

after the experiment was initiated, while by simulation it was 14 °C; this is the largest variation observed when comparing the data. The curve obtained by simulation follows a polynomial trend of fifth order, with an R2 coefficient of 0.99.

Curves of data of thickness of ice obtained by simulation and experimentally are shown in Figure 7b. It can be observed a variation in the first hour of operation, with a maximum difference of thickness of ice of 2 mm; this is because the generation of ice started 10 minutes after the equipment was turned on, while by simulation it started half hour later. The curve follows a polynomial trend of third order, with an R2 coefficient of 0.998.

On the other hand, Figure 7c presents data of variation of temperature of the surface layer between the evaporator and the water (T_{s1}), obtained by simulation and experimentally. Two equations need to be used to define the change in this temperature, the first defining the variation of temperature in the cooling and change of phase, while the second equation indicates subcooling. The curves presented follow polynomial trends of third and sixth order, with an R2 coefficient of 0.996.

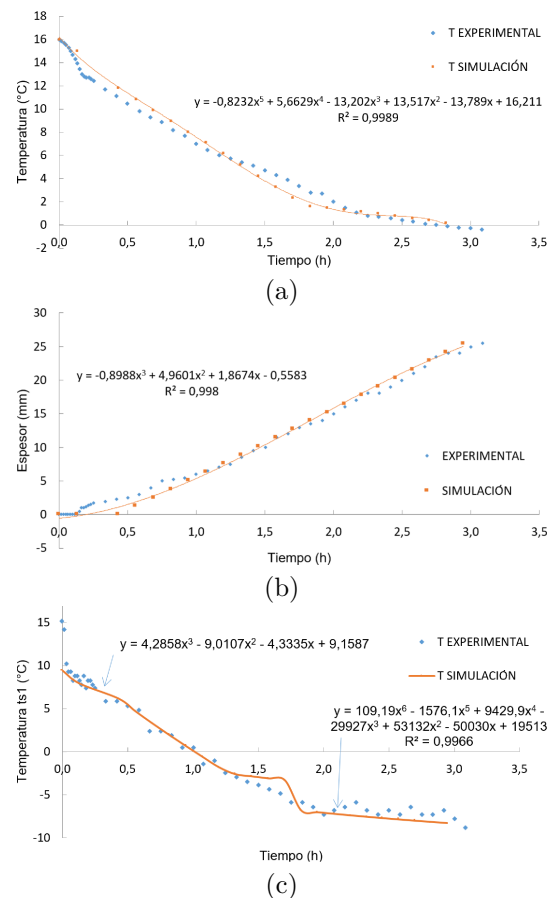


Figure 7. Data of temperature and thickness of ice obtained by simulation and experimentally: a) Temperature of the water vs. time. b) Thickness of ice vs. time c) Temperature of the surface layer vs. time.

A particular situation occurs with the plot of velocity of formation of ice in time shown in Figure 8. Experimentally, the thickness of ice increases at larger velocity and stabilizes after one hour, while by simulation a velocity increasing in time was expected, starting after half hour of equipment operation. This difference is due to instabilities in the process of formation of ice. After one hour has elapsed, the two curves get closer indicating equality. From the third hour of equipment operation, the velocity of formation of ice tends to remain with minimum variations (approximately 1 mm per hour)

Table 2 summarizes the results obtained in the different experiments during 3 hours. It was determined the error in the simulation data (S) with respect to the obtained experimentally (E), remarking the following:

The differences observed when comparing the data of final temperature of water and thickness of ice obtained by simulation and experimentally, are due to the instability occurred in the process of formation of ice during the first hour of experiment. For the final temperature of the water, the percentage of error calculated is in the range from 1.78 % to 80 %, which is

large because the values obtained by simulation indicated smaller temperatures; the mathematical model considered a constant variation of temperature in the condenser, which is very similar to the variation of temperature observed in the tests carried out during the morning and the afternoon, but in tests performed at night the variation of temperature decreased significantly obtaining final temperatures of water higher than expected. For the data of thickness of ice generated, the percentage of error calculated varies in the range from 0.39 % to 15.24 %.

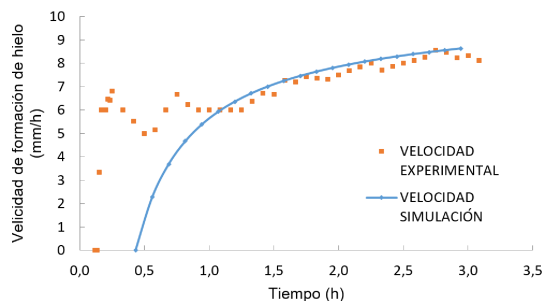


Figure 8. Velocity of formation of ice vs. time.

Table 2. Results of calculations carried out for the different practices in 3 hour

Parameters	Values											
	E	S	% Error	E	S	% Error	E	S	% Error	E	S	% Error
Initial temperature of water (°C)	16 °C			21,5 °C			18 °C			19,4 °C		
Final T of water (°C)	-0,4	-0,41	1,78	1,1	0,93	15,45	-0,5	-0,1	80	1	1,78	78
Ts1 (°C)	-7,82	-8,27	5,75	-7,33	-5,87	19,99	-6,35	-7,59	19,45	-7,82	-7,67	1,92
Thickness (mm)	25,5	25,4	0,39	21	17,8	15,24	23,5	22,9	2,55	23	22,9	0,43
Velocity of formation of ice (mm/h)	8,27	8,63	4,32	6,81	5,99	12,12	7,62	7,59	0,41	7,26	7,52	3,54
Total Q (W)	905,38	1139,28	25,83	858,55	1139,93	32,77	901,05	1140,45	26,57	869,93	1139,93	31,04
Work by compressor (W)	168,64	163,93	2,79	172,69	204,2	18,25	178,58	163,93	8,21	185,95	163,93	11,84
Energy consumed (Wh)	519,99	491,8	5,42	532,45	612,6	15,05	550,64	491,79	10,69	588,85	491,79	16,48
COP	5,97	7,02	17,7	5,85	5,63	3,7	5,94	7,02	18,26	5,85	7,02	20,04
Cooling efficiency (%)	91,39	74,22	18,79	84,02	71,27	15,17	91,87	74,22	19,21	86,19	74,22	13,88
Time at 1 °C (h)	2,17	2,2	1,7	3,08	3,17	2,81	2,5	2,36	5,6	3,08	2,66	13,73
Thickness at 1 °C (mm)	17	17,8	4,71	21	21	0	19	18,1	4,74	22,5	19,77	12,13

A relevant difference is observed in the percentage of error of the refrigeration capacity to be removed, obtained by simulation and experimentally. Since the value given in the product catalog was used in the simulation, this is an optimal refrigeration capacity for selection, but it is not the real one; an important difference is observed when compared with the real value, since the percentage of error varies from 25.83 % to 32.77 %.

The percentages of error evaluated for the velocity of formation of ice, work of the compressor, energy consumed, COP and refrigeration efficiency did not exceed 20 %. For the conducted parametric study, the margin of error obtained is acceptable.

4. Conclusions

It was developed a mathematical model based on the study of the thermal cycle and existent heat transfer, and a programming code for simulation in Guide of MATLAB. The program created enables varying the data of the equipment, operation, ambient and working fluid, with the purpose of observing the change in efficiency, power consumed and its interaction in time. The curves obtained by simulation were validated comparing them with the curves obtained with experimental data, and evaluating the percentage of error between these results.

The main parameters that intervened in the process of formation of ice and storage of thermal energy, were the ambient conditions of the place where the

equipment was installed and the temperature of the water used. The equipment installed in Riobamba decreased its refrigeration capacity to the one presented in the catalog, due to the barometric pressure of the place and the ambient temperature in sunny days.

The instability observed in the process of formation of ice during the first hour of the experiment, directly intervenes in the final temperature of the water. As the formation of ice starts 15 minutes before the time observed by simulation, more heat than the calculated was removed, obtaining a final temperature of water smaller than the observed by simulation. The final temperature of the water varied in the range from 1.1 °C to -0.4 °C in 3 hours.

The greatest efficiency found and the smallest energy consumption were observed in experiments carried out at night, when the ambient temperatures decrease, thus decreasing the thermal load and improving the efficiency of the condenser, which directly influences on the efficiency of the equipment. For operation at night with the water temperature equal to 16 °C.

References

- [1] A. Saito, "Recent advances in research on cold thermal energy storage," *International Journal of Refrigeration*, vol. 25, no. 2, pp. 177–189, 2002. [Online]. Available: [https://doi.org/10.1016/S0140-7007\(01\)00078-0](https://doi.org/10.1016/S0140-7007(01)00078-0)
- [2] I. Dincer, "On thermal energy storage systems and applications in buildings," *Energy and Buildings*, vol. 34, no. 4, pp. 377–388, 2002. [Online]. Available: <http://www.sciencedirect.com/science/article/pii/S0378778801001268>
- [3] J. H. M. Neto and M. Krarti, "Parametric analysis of an internal-melt ice-on-coil tank," *ASHRAE*, vol. 103, no. 2, pp. 322–333, 1997. [Online]. Available: <https://bit.ly/2PyxJ3r>
- [4] S. Sanaye and A. Shirazi, "Thermo-economic optimization of an ice thermal energy storage system for air-conditioning applications," *Energy and Buildings*, vol. 60, pp. 100–109, 2013. [Online]. Available: <https://doi.org/10.1016/j.enbuild.2012.12.040>
- [5] O. J. Venturini, M. d. S. Valente de Almeida, and E. Silva, "Optimización de un sistema de termoacumulación en un tanque de hielo con expansión directa," *Asociación Brasileña de Ingeniería y Ciencia Mecánicas*, 1999. [Online]. Available: <http://bit.ly/2WaawaN>
- [6] M. H. Rahdar, A. Emamzadeh, and A. Ataei, "A comparative study on pcm and ice thermal energy storage tank for air-conditioning systems in office buildings," *Applied Thermal Engineering*, vol. 96, pp. 391–399, 2016. [Online]. Available: <https://doi.org/10.1016/j.applthermaleng.2015.11.107>
- [7] Z. Kang, R. Wang, X. Zhou, and G. Feng, "Research status of ice-storage air-conditioning system," *Procedia Engineering*, vol. 205, pp. 1741–1747, 2017, 10th International Symposium on Heating, Ventilation and Air Conditioning, ISHVAC2017, 19-22 October 2017, Jinan, China. [Online]. Available: <https://doi.org/10.1016/j.proeng.2017.10.020>
- [8] P. A. Intemann and M. Kazmierczak, "Heat transfer and ice formations deposited upon cold tube bundles immersed in flowing water. i. convection analysis," *International Journal of Heat and Mass Transfer*, vol. 40, no. 3, pp. 557–572, 1997. [Online]. Available: [https://doi.org/10.1016/0017-9310\(96\)00121-4](https://doi.org/10.1016/0017-9310(96)00121-4)
- [9] M. H. Rahdar, M. Heidari, A. Ataei, and J.-K. Choi, "Modeling and optimization of r-717 and r-134a ice thermal energy storage air conditioning systems using nsga-ii and mopso algorithms," *Applied Thermal Engineering*, vol. 96, pp. 217–227, 2016. [Online]. Available: <https://doi.org/10.1016/j.applthermaleng.2015.11.068>
- [10] J. Pu, G. Liu, and X. Feng, "Cumulative exergy analysis of ice thermal storage air conditioning system," *Applied Energy*, vol. 93, pp. 564–569, 2012, (1) Green Energy; (2) Special Section from papers presented at the 2nd International Energy 2030 Conf. [Online]. Available: <https://doi.org/10.1016/j.apenergy.2011.12.003>
- [11] Y. Li, C. Yang, Z. Yan, B. Guo, H. Yuan, J. Zhao, and N. Mei, "Analysis of the icing and melting process in a coil heat exchanger," *Energy Procedia*, vol. 136, pp. 450–455, 2017, 4th International Conference on Energy and Environment Research ICEER 2017. [Online]. Available: <https://doi.org/10.1016/j.egypro.2017.10.302>
- [12] ARCONEL. (2019) Balance nacional de energía eléctrica. [Online]. Available: <http://bit.ly/2PiU2eS>
- [13] CONELEC. (2013) Plan maestro de electrificación 2013-2022. aspectos de sustentabilidad y sostenibilidad social y ambiental. [Online]. Available: <http://bit.ly/33UgUFA>
- [14] S. Sanaye and A. Shirazi, "Four e analysis and multi-objective optimization of an ice thermal energy storage for air-conditioning applications," *International Journal of Refrigeration*, vol. 36, no. 3, pp. 828–841, 2013. [Online]. Available: <https://doi.org/10.1016/j.ijrefrig.2012.10.014>

- [15] X. Song, T. Zhu, L. Liu, and Z. Cao, "Study on optimal ice storage capacity of ice thermal storage system and its influence factors," *Energy Conversion and Management*, vol. 164, pp. 288–300, 2018. [Online]. Available: <https://doi.org/10.1016/j.enconman.2018.03.007>
- [16] H. H. Sait, "Experimental study of water solidification phenomenon for ice-on-coil thermal energy storage application utilizing falling film," *Applied Thermal Engineering*, vol. 146, pp. 135–145, 2019. [Online]. Available: <https://doi.org/10.1016/j.applthermaleng.2018.09.116>
- [17] G. D. Shinde and P. R. Suresh, "A review on influence of geometry and other initial conditions on the performance of a pcm based energy storage system," *International Journal of Thermal Technologies*, vol. 4, no. 3, pp. 214–222, 2014. [Online]. Available: <http://bit.ly/31KAL8A>
- [18] R. A. Jordan, L. A. B. Cortez, V. Silveira Jr., M. E. R. M. Cavalcanti-Mata, and F. D. de Oliveira, "Modeling and testing of an ice bank for milk cooling after milking," *Engenharia Agrícola*, vol. 38, pp. 510–517, 08 2018. [Online]. Available: <https://bit.ly/2E6ZACD>
- [19] K. A. R. Ismail, M. M. Gonçalves, and F. A. M. Lino, "Solidification of pcm around a finned tube: Modeling and experimental validation," *Journal of Basic and Applied Research International*, vol. 12, no. 2, pp. 115–128, 2015. [Online]. Available: <http://bit.ly/3410fjU>
- [20] R. P. Guapulema Maygualema and E. A. Jácome Domínguez, "Diseño y construcción de un generador de hielo tubular para laboratorio," 2013. [Online]. Available: <https://bit.ly/2RETbq9>
- [21] H. H. Sait, A. Hussain, and A. M. Selim, "Experimental investigation on freezing of water falling film on vertical bank of cold horizontal tubes," *Journal of thermal science and engineering applications*, vol. 4, no. 4, p. 041006, 2012. [Online]. Available: <https://doi.org/10.1115/1.4006314>
- [22] F. Wang, C. Liang, M. Yang, C. Fan, and X. Zhang, "Effects of surface characteristic on frosting and defrosting behaviors of fin-tube heat exchangers," *Applied Thermal Engineering*, vol. 75, pp. 1126–1132, 2015. [Online]. Available: <https://doi.org/10.1016/j.applthermaleng.2014.10.090>
- [23] H. G. Ramírez-Hernández, F. A. Sánchez-Cruz, F. J. Solorio-Ordaz, and S. Martínez-Martínez, "An experimental study of heat transfer on a tube bank under frost formation conditions," *International Journal of Refrigeration*, vol. 102, pp. 35–46, 2019. [Online]. Available: <https://doi.org/10.1016/j.ijrefrig.2019.01.031>
- [24] S. K. Wang, *Handbook of Air Conditioning and Refrigeration*, mcgraw-hill ed., 2000. [Online]. Available: <http://bit.ly/344CVlj>
- [25] ASHRAE, *ASHRAE handbook : fundamentals*, 2001. [Online]. Available: <https://bit.ly/2LMExtf>
- [26] Y. Çengel and M. Boles, *Termodinámica*, 2015. [Online]. Available: <https://bit.ly/2E5v8J3>
- [27] J. P. Holman, *Transferencia de calor*, 1998. [Online]. Available: <https://bit.ly/2PdyO1N>
- [28] F. Taboas Touceda, "Estudio del proceso de ebullición forzada de la mezcla amoniaco/agua en intercambiadores de placas para equipos de refrigeración por absorción," Ph.D. dissertation, 2006. [Online]. Available: <https://bit.ly/34b58Xk>